Astronomical and Astrophysical Transactions (*AApTr*), 2019, Vol. 31, Issue 3, pp. 267–280,
ISSN 1055-6796, Photocopying permitted by license only, ©Cambridge Scientific Publishers

Dynamics of the polarization sign during the solar flare on 2013-10-28

A.V. Shain[1,*], A.S. Morgachev[1,2], V.F. Melnikov[1]

[1] *Pulkovo Observatory (Russian Academy of Sciences), Saint Petersburg, Russia*
[2] *Radiophysical Research Institute of Lobachevsky State University, Nizhny Novgorod, Russia*

Received 1 October, 2018

In our work we consider microwave spatial and temporal polarization inversion during a solar flare of class X1.0 on October 28, 2013. The QT effect is shown to be important for the polarization inversion. In a constructed model, the temporal inversion of the microwave burst polarization has been attributed to the effect of ignition of several flaring loops with different orientations relative to the observer.

Keywords: Sun: flares, microwave, polarization

1 Introduction

While propagating in a solar magnetoactive plasma, radio waves are split into circularly polarized ordinary (O) and extraordinary (X) modes. In the extraordinary wave, the electric field vector rotates in the direction of rotation of an electron, but in the ordinary wave against the rotation of the electron. The radio wave mode from the radio source is usually determined by the type of polarization of the received wave (right-hand R or left-hand L) and the direction of the magnetic field in the radio source (**to** the observer or **from** the observer) if this direction is known. For example, the wave from a radio source above an N-polarity sunspot (the magnetic field is directed **to** the observer) located in the central part of the solar disk is extraordinary if the received radiation is R-polarized and vice versa if the received radiation is L-polarized. Other things being equal, the radio wave from the source above the S polarity spot is ordinary if the received radiation is R-polarized, and extraordinary if the received radiation is L-polarized.

During solar flares, microwave sources are associated with gyrosynchrotron radiation of mildly relativistic electrons. It is usually expected that this radiation is polarized in the extraordinary mode (Dulk and Marsh 1982). However, analysis of the microwave polarization from some sources during solar flares leads to the conclusion

*Email: alexandershain.5@gmail.com

about polarization in the ordinary mode (Altyntsev et al. 2008; Morgachev et al. 2014, 2016; Shain et al. 2017). The conclusion about the dominance of the ordinary mode of radiation is made when the sign of the polarization of the received radiation from the source is opposite to the sign of the magnetic field polarity in the source or when the polarization sign from the source varies with time (Morgachev et al. 2016).

There are three most probable explanations for such events with the polarization inversion. The first explanation is based on the theoretical fact of the polarization inversion in the presence of longitudinal pitch-angular anisotropy of emitting electrons (Fleishman & Melnikov 2003). Such a scenario was used to interpret the microwave source polarization inversion in works of Altyntsev et al. (2008); Morgachev et al. (2014). In Morgachev et al. (2015), the non-stationary kinetics of the accelerated electrons in the flare loop was simulated and the obtained results were compared with the spatial dynamics of the observed radiation. The modeling allowed to explain not only the spatial inversion of the polarization sign in the flare loop, but also its temporal variation and inversion.

The second explanation is based on the assumption of gyrosynchrotron radiation from positron fluxes, which can be born during powerful solar flares (Fleishman et al. 2013). The direct evidence of such a process could be an observation of the line 511 keV from the annihilation of electrons and positrons. One of the most probable events in which strong gyro-synchrotron radiation was observed from positrons, is the flare of SOL2003-03-13 (Fleishman et al. 2013). At the same time, Morgachev et al. (2016) noted that the observed polarization features of this flare are rather fully explained by the specific pitch-angle anisotropy of the accelerated electrons. The above mechanisms can explain the observation of the ordinary mode of emisson at high frequencies of the microwave radiation, for example, at the frequency Nobeyama RadioHeliograph 17 GHz and above.

The so-called quasi-transverse propagation effect (QT) is used as the third polarization reversal mechanism. For it, the geometry of the magnetic field in the path of propagation of the radio wave is important. The effect of quasi-transverse propagation in the lower corona under the condition of a plasma concentration $n = 10^8$ cm^{-3} and a characteristic scale of the variation of the field $5 \cdot 10^9$ cm/rad at a frequency of 17 GHz is possible for a sufficiently strong magnetic field of the order of 140 G (Cohen 1960; Zheleznyakov & Zlotnik 1963). The QT-effect has long been known, and has been repeatedly applied to solar radio emission (Cohen 1961; Cohen & Dwarkin 1961; Takakura 1961; Alissandrakis & Preka-Papadema 1984; Su & Huang 2003; Huang & Nakajima 2009; Shain et al. 2017). In these works, either simplest models of the coronal magnetic field, or data on the projection of the photospheric magnetic field on the line of sight have been applied. Only in the recent paper (Altyntsev et al. 2017) the QT-effect was modeled and explained, based on the SDO/HMI data on the photosphere vector magnetic field.

The purpose of this paper is to study, not only spatial, but also temporal polarization inversion observed in some flares. We analyze a specific flare with a polarization inversion and propose a model in which a change in the sign of polarization during a burst is possible due to ignition of new flaring loops with slightly different geometry. The basis for this model is a recent study by Kuznetsov et al. (2016), in which it is shown that the pulsating X-ray emission of solar flares can be associated with the ignition of new flaring loops.

2 Observations and data analysis

Flare 01:59UTC 28-10-2013 was selected for the study from the Nobeyama Radioheliograph event catalog (Fig. 1). The flare had power class X1.0 according to the GOES classification and occurred near the Sun western limb, its heliographic coordinates N05W69. The peak of the total radio flux at 17 GHz during the flare was 3000 SFU.

Nobeyama Radioheliograph (NoRH) gives a possibility to obtain spatially resolved data about brightness temperature (Stocks I parameter) at two frequencies, 17 and 34 GHz, simultaneously with high angular ($10''$ and $5''$, respectively) and temporal (0.1 s) resolution. At 17 GHz it also provides polarization Stocks V parameter with the same resolution as for Stocks I. This provides a chance to study the brightness distribution of intensity and polarization having the information on microwave spectrum slope $\alpha = \log(I_{34}/I_{17})/\log(34/17)$, and, therefore, on the optical thickness in different parts of a flaring loop.

At the very beginning of the microwave burst, the entire flare loop was right-hand polarized at 17 GHz, $V = R - L > 0$. However, immediately after the maximum

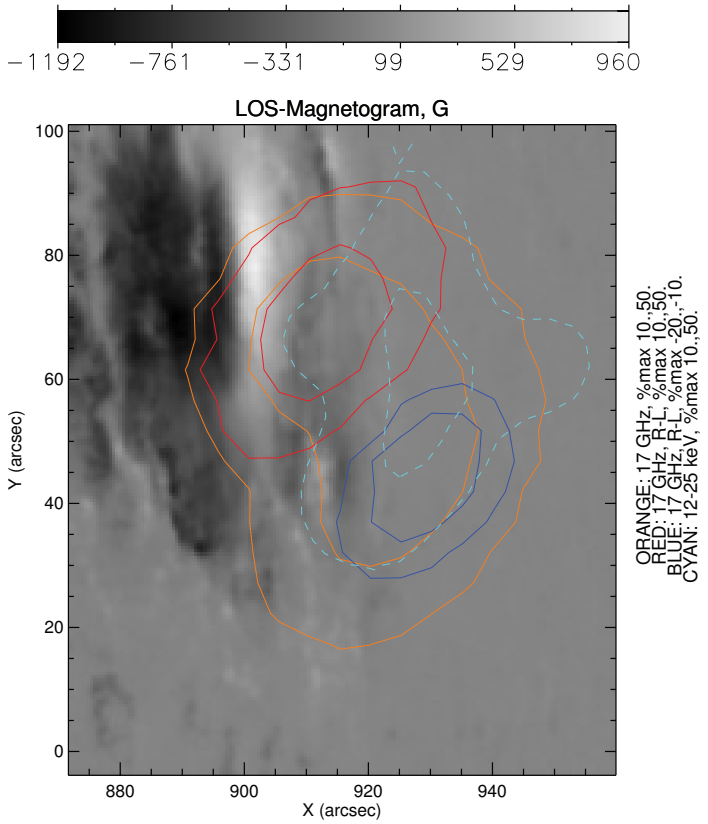


Figure 1 NoRH 17 GHz $I_R - I_L$ (red and blue) and $I_R + I_L$ (orange), RHESSI 12–25 keV count rates (cyan) contours on the line of sight SDO/HMI magnetogram. The contours correspond to the moment just after the intensity maximum ($\approx$ 01:59:50 UT).

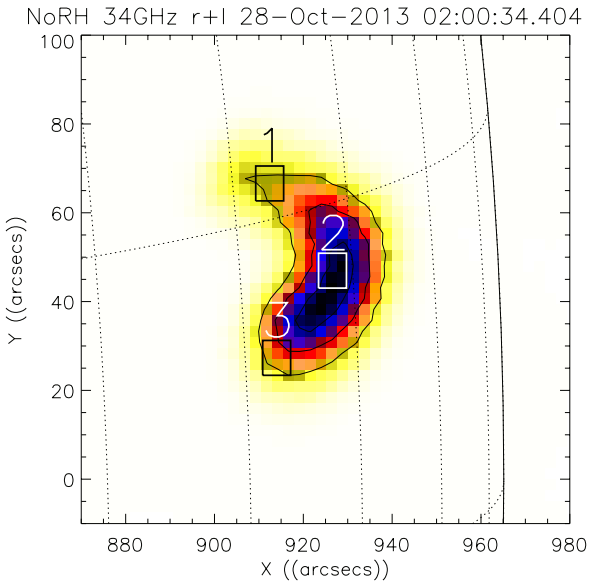


Figure 2 Location of boxes on the 34 GHz $I_R + I_L$ image taken at the burst intensity maximum.

intensity in the central (Box 2) and southern (Box 3) parts of the loop, the polarization sign reversed to a negative one, $V = R - L < 0$ (see Figs 2 and 3).

When analyzing the features of microwave radiation during the flare, the NoRH data gave rise to suspicion of the dominance of the ordinary mode of microwave radiation in the northern part of the flare loop (Box 1 in Fig. 2). This suspicion is based on the fact that the northern foot of the loop rests on the southern (negative) polarity of the photospheric magnetic field (see Fig. 1), and the polarization of the observed radiation at 17 GHz is positive: $V = R - L > 0$. Domination of the ordinary mode could be attributed to the large optical thickness of this part of the loop (Dulk & Marsh 1982). However, the slope of the frequency spectrum of the radiation between 17 and 34 GHz in this part of the radio source is negative, especially at the beginning of the burst: $\alpha = -3...-2$, which indicates that the radio source was optically thin. Hence, the reason must be different. It is interesting that the degree of positive polarization in Box 1 decreases noticeably (from 12% to 4%) during the rise phase of the burst intensity (01:58–02:00 UT, Fig. 3). This usually occurs when the optical thickness of the source grows because of the accumulation of energetic electrons in the loop. This fully agrees with the dynamics of the slope of the spectrum (Fig. 3, bottom panel): in the rise phase, index α decreases in absolute value, and increases during the decay phase due to a decrease in the optical thickness (Kuznetsov & Melnikov 2012).

Another interesting feature of the investigated flare loop is the polarization behavior in the sources of Box 2 and Box 3 (loop top and south foot) immediately after the maximum burst intensity (Fig. 3, third panel from above). At the top of the loop (Box 2), the polarization changes its sign from positive to negative fairly fast, in less than 20 s. In the south foot (Box 3), the degree of polarization also quickly becomes

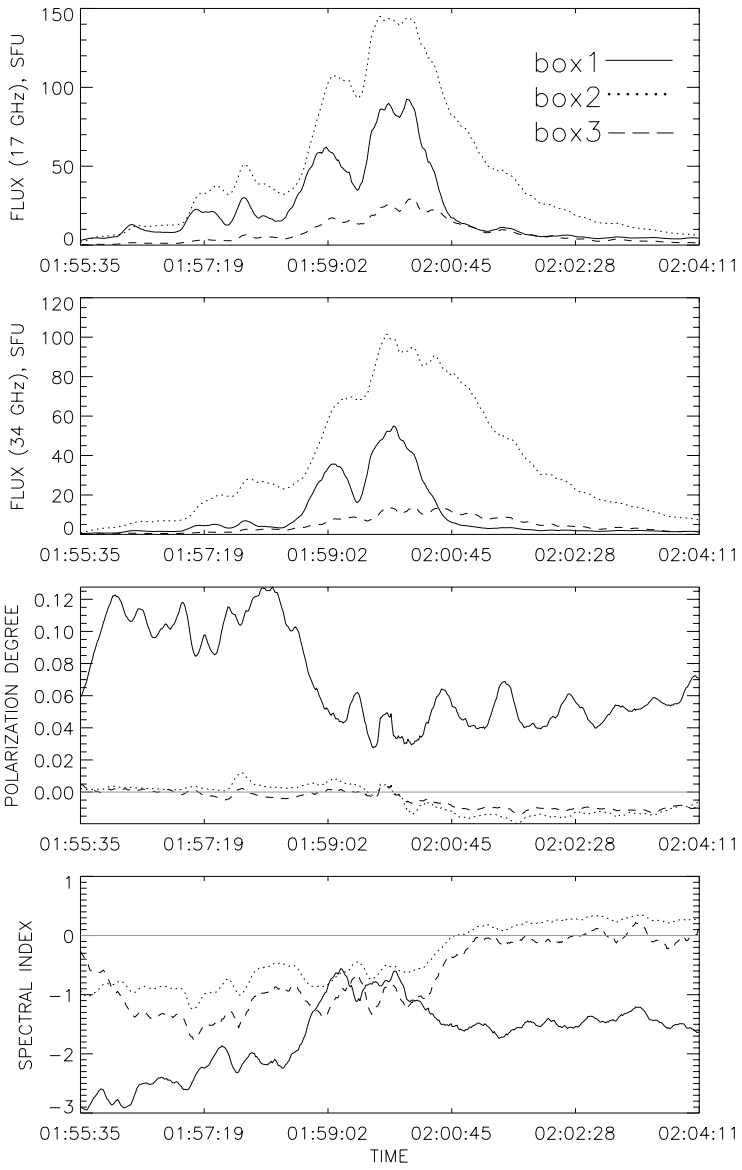


Figure 3 Evolution of flux $I_R + I_L$, polarization degree $(I_R - I_L)/(I_R + I_L)$ and spectral index $\alpha = \log(I_{34}/I_{17})/\log(34/17)$ in Boxes 1, 2, 3 (see Fig. 2) during the event.

negative. We note that the positive and nearly zero polarization in these places of the flare loop is in complete agreement with the model calculations of the magnetic field geometry given below in the section "Modeling". In this case, the positive sign of the observed polarization corresponds to extraordinary mode. That is, changing the sign of polarization to negative corresponds to inversion into ordinary mode.

What is the reason for the temporary inversion of the polarization sign at the top and south foot of the flare loop? Obviously, a large increase in the optical thickness to $\tau > 1$ cannot be the cause of inversion, since in the decay phase in the intensity of the burst, the optical thickness of these sources should, on the contrary, decrease rather than grow. The flattening of the frequency spectrum observed in the decay phase (Fig. 3, bottom panel) is quite typical and is connected either with the flattening of the energy spectrum of the electrons after the end of the intensive injection (see Melnikov & Magun 1998) or with the enhancement of the Razin effect due to the increasing density of plasma in the loop due to evaporation of the chromosphere (Melnikov et al. 2008; Kuznetsov & Melnikov 2012). Both of these factors can not lead to the dominance of ordinary mode. The appearance of a stream of energetic electrons with a longitudinal pitch-angular distribution at the top of the loop could, in principle, lead to an increase and dominance of the ordinary mode in gyrosynchrotron radiation. However, in this explanation there is a weak point: with longitudinal anisotropy at the top of the loop, it is impossible to obtain a peak of the brightness of the GS radiation in the upper part of the loop, it will necessarily be near the footpoints (Melnikov et al. 2002).

We propose a model in which a change in the sign of polarization during a burst is possible due to the ignition of new flare loops with slightly different geometry. The basis for this model is a recent study by Kuznetsov et al. (2016), in which it is shown that the pulsating X-ray emission of solar flares can be associated with the successive ignition of new loops.

The possibility of such ignition of multiple loops is confirmed by multiple radiation pulses, visible on the temporal profiles of the microwave radiation of the analyzed flare (Fig. 3). Similar and even more pronounced pulsations can also be observed in hard X-ray radiation (Fig. 4). These facts indicate that, probably, there is an ignition of

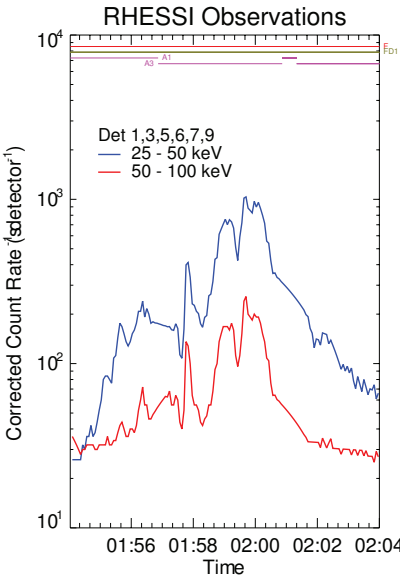


Figure 4 RHESSI 25–50 keV and 50–100 keV count rates near the flare peak.

new loops which are not resolved by the radioheliograph. This can also be indicated by abrupt changes in the degree of polarization near the peaks of the burst.

To confirm the complex spatial structure of the microwave burst, ultraviolet images recorded on AIA/SDO were used in the "hot" line 94 Å indicating a plasma heated to temperatures of the order of 10^7 K. To determine the location of the loop, X-ray data from the RHESSI spacecraft in the channels 12–25 keV and 50–100 keV were also used. These images were synthesized using the Pixon algorithm in the Solarsoft Hessi Imaging Software package.

3 Modeling coronal magnetic field and microwave emission

For a detailed simulation of the microwave radiation of the flare, we reconstructed the spatial structure of the coronal magnetic field from vector magnetograms. A vector magnetic field at photosphere level was obtained from the 12-minute SDO / HMI data. It was used as a boundary condition for the restoration of the coronal magnetic field. A nonlinear force-free field approximation for extrapolation was chosen. We used the optimization method (Wheatland et al. 2000) implemented in a program developed by Rudenko & Myshyakov (2009) and adapted for GX Simulator.

The criterion for the succesful restoration was the approximate coincidence of the loop model image with the data on the observed microwave intensity distribution (Fig. 5) as well as the X-ray intensity distribution. To visualize the loops and calculate the spatial distribution of the characteristics of microwave (gyro-synchrotron) emission, and to simulate the propagation of this radiation in the corona, the Solar Soft GX Simulator package was used (Nita et al. 2015). The created 3D coronal model had the dimension $128 \times 128 \times 64$ voxels with a step of 1500 km. The parameters for modeling the corona and flare loops are presented in Shain et al. (2017). They are standard for the GX Simulator program.

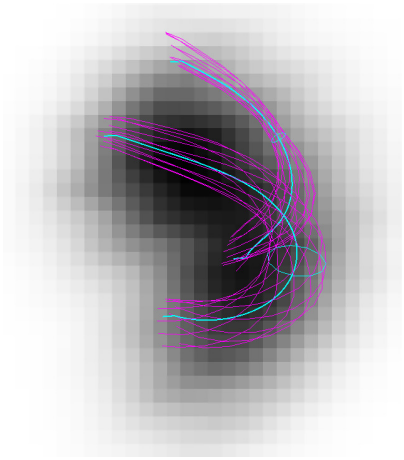


Figure 5 GX Simulator screen with studied model of two loops and 17 GHz $I_R + I_L$ reference map.

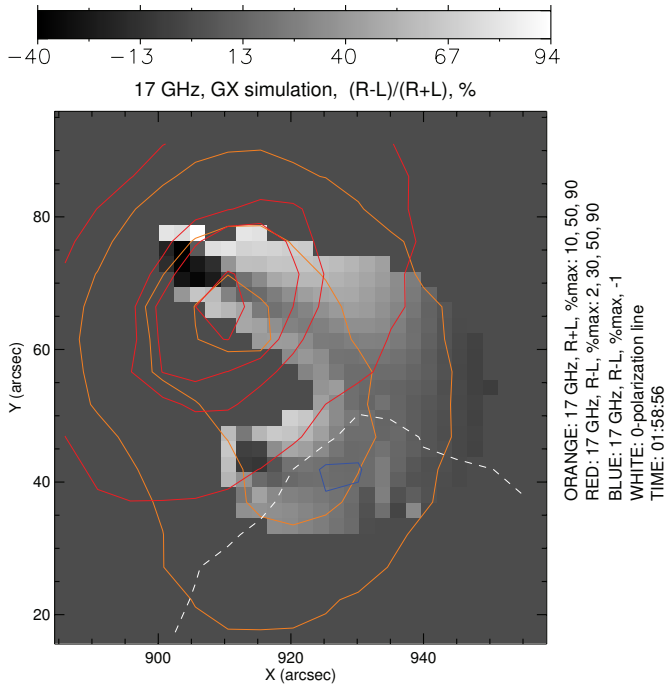


Figure 6 The closest loop simulated polarization degree with overlayed contours of 17 GHz, $I_R + I_L$ (red and blue), $I_R + I_L$ (orange), which are taken at the moment 01:58:56 UT. The white dashed line is the zero polarization line.

In order to explain the dynamics of the sign of the polarization of the microwave flare under consideration without attracting special hypotheses on the dynamics of accelerated electrons in a single flare loop, we assumed the existence of two separate consecutive illuminated loops. Here are some parameters of these model loops. The loop closest to the observer has the following characteristic values of magnetic field: $B = 210$ G, in the northern footpoint 1560 G, in the southern footpoint 730 G. The magnetic field of the remote loop takes the following values: at the top $B = 130$ G, in the northern footpoint 480 G, in the southern footpoint 80 G. The height of the loops does not exceed 25 Mm.

In Fig. 6 we show the simulated microwave source corresponding to the loop closest to the observer. Almost the whole source, from its northern to southern foot, has a positive polarization sign. This corresponds to the observations in the beginning of the burst rise phase. Thus, for a stationary emission of an extraordinary mode of microwave radiation, a loop of this geometry is incapable to explain the change in the polarization sign which happens later as shown by the overlayed NoRH polarization contours taken at the moment 01:58:56 UT. At this moment we can see a weak negative polarization dominance of microwave radiation (the blue contour in the southern part of the loop) to demonstrate the above statement.

The northern leg of a nearby flare loop lies in the region of a strong magnetic field of 1560 G. In this case, the radiation from this part of the loop passes through a region

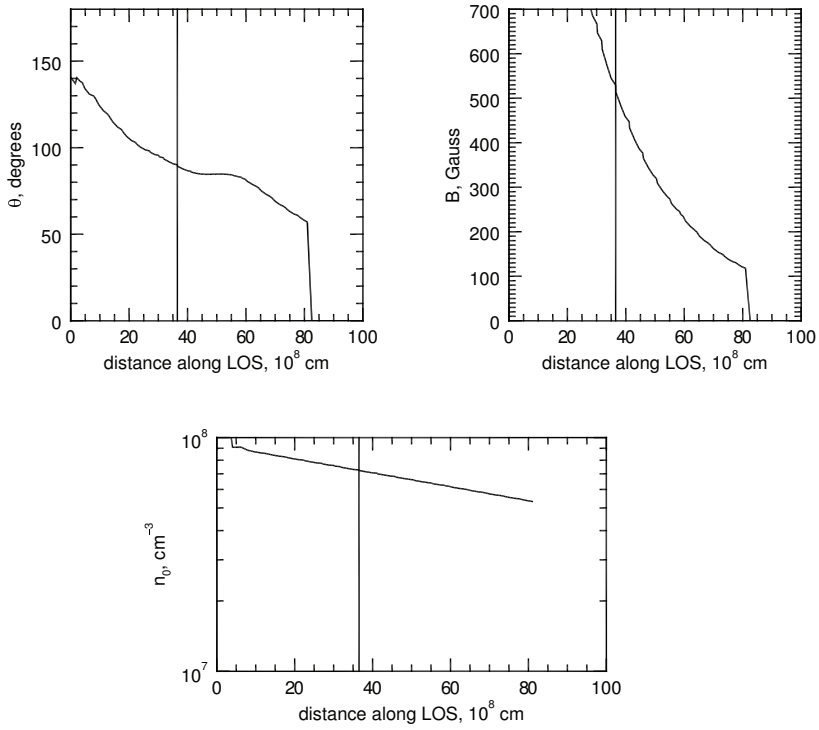


Figure 7 Magnetic field and corona parameters along the ray path from the northern footpoint of the closest loop. The vertical line at each panel shows the distance where magnetic field is transverse to the ray path (LOS).

of a strong transverse magnetic field (Fig. 7), for which the critical frequency of the QT-effect is noticeably higher than 17 GHz. This means that despite the fact that an extraordinary mode is emitted in this source, the observer will see this radiation with inverted polarization. Thus, the ordinary mode, observed stationary in the northern leg of the microwave loop, is explained by the QT-effect.

Further we assume that the closest loop radiates in an optically thin regime. As noted above, the data of the radioheliograph Nobeyama allow us to make such an assumption (see Fig. 3). In Fig. 8, it can be seen that the loop, far from the observer, near its top in the southern leg has a negative sign of polarization. This can explain the observed sign of the microwave radiation polarization at the maximum of the burst. It can be noted that in this model the radiation from the southern leg of the far loop passes through 3 QT-regions (Fig. 9). The first of them has a weak magnetic field of 120 G and the rapid rate of change in its direction. Therefore, in this region there is no QT-effect and there is no change in the polarization sign. The action of the following two regions of the transverse field along the paths of the rays from the southern leg of the far loop compensate each other without affecting the observed polarization sign.

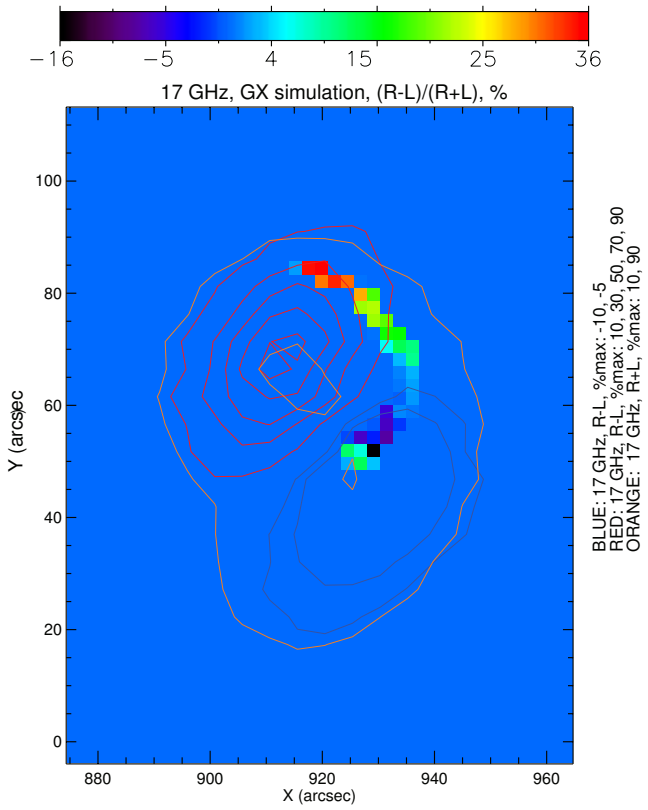


Figure 8 The remote loop simulated polarization degree. As is shown on the color bar, the red color corresponds to the positive polarization sign, and the blue one to the negative sign. The overlaid contours of 17 GHz, $I_R - I_L$ (red and blue), $I_R + I_L$ (orange) show the related distributions of the observed parameters at time 01: 59: 39 UT close to the burst maximum.

Conclusions

In our work we have considered the unusual phenomenon of microwave spatial and temporal polarization inversion which was found during the solar flare of class X1.0 on October 28, 2013 with heliographic coordinates N05 W69.

According to the Nobeyama Radioheliograph data, at the very beginning of the flare, the entire microwave flare loop was right-hand polarized at 17 GHz. For the northern part of the microwave flare loop, this fact is in contradiction with the common expectation which follows from the direction of photospheric magnetic field observed with SDO/HMI, and indicates on the dominance of the ordinary mode microwave emission. After the analysis of the microwave emission properties during the flare along with the restored spatial structure of the coronal magnetic field we made the conclusion that the cause of the polarization inversion in the northern part of the microwave loop is the quasi-transverse propagation effect on the path of radio

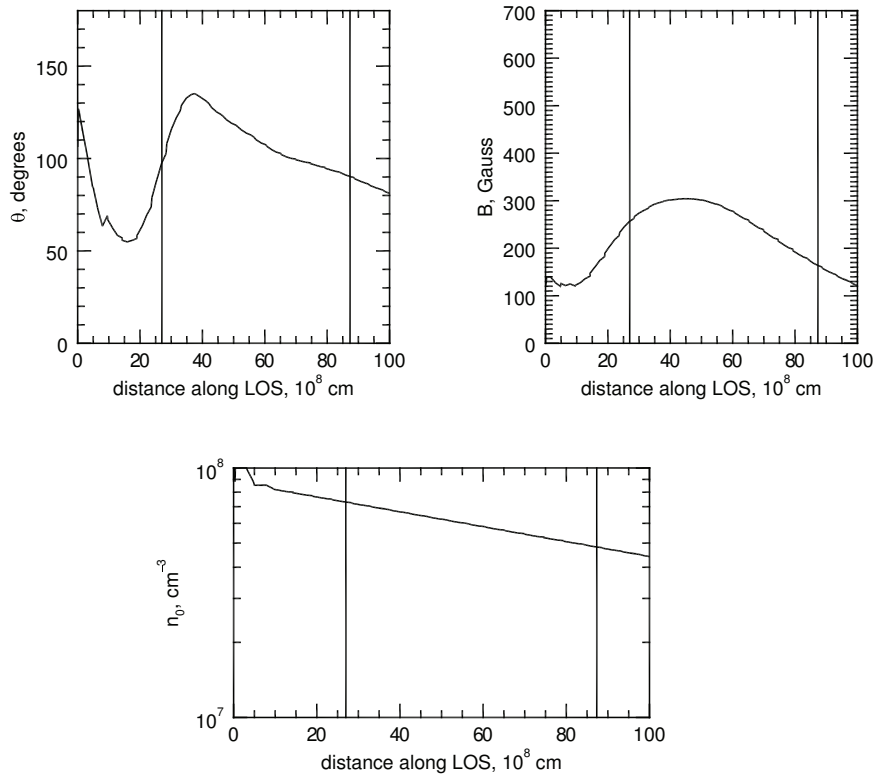


Figure 9 Magnetic field and corona parameters along the ray path from the southern footpoint of the remote loop. The vertical line at each panel shows the distance where magnetic field is transverse to the ray path (LOS).

waves from the loop to an observer. It is shown that other possible mechanisms of the polarization inversion, such as high optical thickness or longitudinal anisotropy of emitting mildly relativistic electrons, are not appropriate here.

Another interesting fact found in this study is the temporal inversion of the polarization sign in the central and southern parts of the visible microwave loop, which happened immediately after the intensity maximum of the burst. In order to explain this fact, we considered a model which assumes that the active flare area is an arcade which consists of at least two separate magnetic loops. The ground for such an assumption is the multi-pulse structure of hard X-ray and microwave emission of the solar flare and the relatively low spatial resolution of microwave observations which do not allow us to see a possible spatial fine structure of the arcade. Our simulation has shown that the changing in the polarization sign during the microwave burst can be caused by the sequential ignition of individual flare loops in the arcade. Within the framework of our model, it is necessary that the acceleration of nonthermal electrons began first of all in the loop closest to the observer, and then in a remote loop. In this case, the combination of the effects, such as the QT-effect, the orientation of the loops relative to each other and to the observer, results in the change of the polarization sign with time.

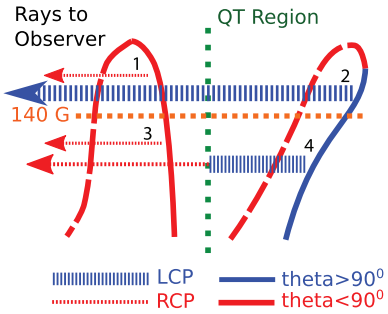


Figure 10 Side view of a flaring arcade seen like a single microwave loop from the Earth. The left loop is ignited first. All shown rays are emitted from the right legs of the loops (imaged by solid lines). Rays 1 and 3 are emitted from the left loop (closer to an observer). Rays 2 and 4 are emitted from the right loop (remote from an observer). Only Ray 4 polarization is affected by the QT effect. This configuration leads to a temporal reversal of the polarization sign near the top of the flaring arcade.

As it was said above, the critical field for the 17 GHz spatially resolved NoRH observations is approximately equal to 140 G (the exact value depends also on the electron number density in the QT domain and on the rate of the magnetic field direction change, Zheleznyakov & Zlotnik, 1963). As a consequence, for the parts of loops in an arcade located in a region with a stronger field, at the legs of loops, the sign of the polarization (R) will not change during a burst due to the QT effect. However, near the top of the microwave loop as the energy release site propagates along the arcade, the sign of the polarization must change (from R to L). Thus, this mechanism should be considered as an alternative to the kinetic mechanism (Morgachev et al. 2014; 2015) which explains the change in the polarization sign of limb flares by progressive change of high energy electrons' pitch-angle distribution.

Acknowledgements

This work was supported by the Russian Foundation for Basic Research, project nos. 17-32-50199_mol–nr (A.V. Shain), 18-02-00856_a (A.S. Morgachev) and 17-52-80064 (V.F. Melnikov). The work was partly carried out with the Solar Data Analysis System operated by the Astronomy Data Center of the National Astronomical Observatory of Japan.

References

Alissandrakis, C.E., Preka-Papadema, P. 1984, Astron. Astrophys. 139, 507
Altyntsev, A.T., Fleishman, G.D., Huang, G.-L., Melnikov, V.F. 2008, Astrophys. J. 677, 1367

Altyntsev, A.T., Meshalkina, N.S., Myshyakov, I.I., Pal'shin, V.D., Fleishman, G.D. 2017, Solar Phys. 292, id. 137
Cohen, M.H. 1960, Astrophys. J. 131, 664
Cohen, M.H. 1961, Astrophys. J. 133, 978
Cohen, M.H., Dwarkin, M.J. 1961, J. Geophys. Res. 66, 411
Dulk, G.A., Marsh, K.A. 1982, Astrophys. J. 259, 350
Fleishman, G.D., Altyntsev, A.T., Meshalkina, N.S. 2013, Pub. Astron. Soc. Japan 65, S7
Fleishman, G.D., Melnikov, V.F. 2003, Astrophys. J. 587, 823
Huang, G., Nakajima, H. 2009, Astrophys. J. 696, 136
Kuznetsov, S.A., Melnikov, V.F. 2012, Geomagn. Aeron. 52, 883
Kuznetsov, S.A., Zimovets, I.V., Morgachev, A.S., Struminsky, A.B., 2016, Solar Phys. 291, 3385
Melnikov, V.F., Magun, A. 1998, Solar Phys. 178, 153
Melnikov, V.F., Gary, D.E., Nita, G.M. 2008, Solar Phys. 253, 75
Melnikov, V.F., Shibasaki, K., Reznikova, V.E. 2002, Astrophys. J. 580, L185
Morgachev, A.S., Kuznetsov, S.A., Melnikov, V.F., 2014, Geomagn. Aeron. (Engl. Transl.), V. 54, p. 933
Morgachev, A.S., Kuznetsov, S.A., Melnikov, V.F., Simes, J.A. 2015, Geomagn. Aeron. (Engl. transl.), 55, 1118
Morgachev, A.S., Melnikov, V.F., Kuznetsov, S.A. 2016, Geomagn. Aeron. (Engl. transl.) 56, 1045
Nita, G.M., Fleishman, G.D., Kuznetsov, A.A., Kontar, E.P., Gary, D.E. 2015, Astrophys. J. 2015, 799, id 236
Rudenko, G.V., Myshyakov, I.I. 2009, Solar Phys. 257, 287
Shain, A.V., Melnikov, V.F., Morgachev, A.S. 2017, Geomagn. Aeron. 57, 988
Su, Y.N., Huang, G.L. 2004, Astrophys. J. 219, 159
Takakura, T. 1961, Publ. Astron. Soc. Jpn. 13, 312
Wheatland, M.S., Sturrock, P.A., Roumeliotis, G. 2000, Astrophys. J. 540, 1150
Zheleznyakov, V.V., Zlotnik, E.Ya. 1963, Astron. Zhurn. 40, 633